Complex beam parameter and *ABCD* law for non-Gaussian and nonspherical light beams

Miguel A. Porras, Javier Alda, and Eusebio Bernabeu

We define the width, divergence, and curvature radius for non-Gaussian and nonspherical light beams. A complex beam parameter is also defined as a function of the three previous ones. We then prove that the *ABCD* law remains valid for transforming the new complex beam parameter when a non-Gaussian and nonspherical, orthogonal, or cylindrical symmetric laser beam passes through a real *ABCD* optical system. The product of the minimum width multiplied by the divergence of the beam is invariant under *ABCD* transformations. Some examples are given.

Key words: Laser beams, laser propagation, matrix optics.

1. Introduction

The propagation and transformation of Gaussian, Hermite–Gaussian (HG), and Laguerre–Gaussian (LG) light beams through paraxial systems are governed by the *ABCD* law.[1–3] However, most of the laser beams are non-Gaussian (non-HG and non-LG). The beams delivered by high-power lasers are often multimodal beams.[4] The transverse modes in unstable resonators are not HG or LG beams. Sometimes non-Gaussian profiles are used for specific applications. For example, super-Gaussian profiles are used for fusion lasers.[5] Other profiles are also used for improving the filling factor inside the laser medium. Most of the time, Gaussian beams are at least weakly distorted in amplitude or phase.[6,7] In addition, a Gaussian beam becomes a lower-quality non-Gaussian and nonspherical beam when it passes through an aperture.[8,9] In such cases the conventional *ABCD* law (valid only for Gaussian, HG, and LG beams) is no longer applicable.

In this paper we introduce non-Gaussian and nonspherical beams into the *ABCD* formalism by using an extension of the concept of the complex beam parameter. In Section 2 we define the width, divergence, and curvature radius for beams with a non-Gaussian intensity profile and nonspherical wave front. Following the research of other authors,[10–12] we will relate the width and divergence with the mean-square deviations (MSD's) of the transversal position and transversal spatial frequency, respectively, for the electric field in the transversal plane. The curvature radius of a nonspherical beam will be defined as the radius of the spherical wave front that best fits the actual wave front. In Section 3 we deduce the transformation laws of the width, divergence, and radius when the beam passes through a purely real *ABCD* system. In Section 4 we define the complex beam parameter by means of a generalization of the corresponding parameter for Gaussian beams and prove that it changes according to the *ABCD* law.

In Sections 2 through 4 we assume that (a) the beam has two orthogonal transversal directions with independent behaviors with regard to its intensity profile and wave front (orthogonal astigmatic beams), so its expression is separable in two functions that only depend on one transversal coordinate; and (b) the magnitudes defined in Section 2, related with mean values of powers of the transversal position and transversal spatial frequency, are well defined.

We raise restriction (a) by extending the results for the orthogonal astigmatic case to beams with cylindrical symmetry (Section 5). We do not deal with general astigmatic beams, even though they could be included if the scalar width, divergence, and radius are generalized to tensor magnitudes.[13]

Restriction (b) excludes an important type of beam: truncated beams. In this case the mean value of the squared transversal frequency is not well defined. Nevertheless, we use one example in Section 6 to

The authors are with the Departamento de Optica, Faculdad de Físicas, Universidad Complutense de Madrid, Cuidad Universitaria s/n 28040, Madrid, Spain. When this research was performed, J. Alda was with the Center for Research in Electro-Optics and Lasers, University of Central Florida, Orlando, Florida 32826.

Received 26 July 1991.
0003-6935/92/306389-14$05.00/0.

suggest how the method can be approximately applied to truncated beams.

2. Width, Divergence, and Radius for Non-Gaussian Beams

The complex beam parameter q of a Gaussian spherical beam at a transversal plane is defined as

$$\frac{1}{q} = \frac{1}{R} - i\frac{\lambda}{\pi\omega^2}, \tag{1}$$

where R is the curvature radius of the spherical wave front, ω is the Gaussian width (the distance at which the intensity is e^{-2} times that on the axis), and λ is the wavelength. More complicated laser beams have neither spherical wave fronts nor points of intensity decay related to the width. Therefore, there are no complex beam parameters, in the usual sense, for non-Gaussian (HG and LG) beams. In addition, the complex beam parameter given by Eq. (1) does not have a clear physical meaning for higher-order HG and LG modes because ω is not their width. To define the complex beam parameter for other types of beams, we must first establish what we understand about the width and the radius of a beam with a non-Gaussian intensity profile and a nonspherical wave front.

Because a laser beam is concentrated on a finite region of the transversal plane, its width can always be measured in some way. The most standard and usual mathematical expression for this magnitude is the MSD. We define the width of a laser beam at a typical plane as the MSD of its intensity profile. In the case of orthogonal astigmatic beams, the field is separable in two orthogonal one-dimensional components. If the amplitude distribution in one of these transversal directions is denoted by $\Psi(x)$, then the width $\omega(\Psi)$ of the beam is given by

$$\begin{aligned}\omega(\Psi) &= 2\left\{\frac{\int_{-\infty}^{\infty}\Psi\Psi^*[x - x(\Psi)]^2\mathrm{d}x}{I(\Psi)}\right\}^{1/2} \\ &= 2\left[\frac{\int_{-\infty}^{\infty}\Psi\Psi^* x^2\mathrm{d}x}{I(\Psi)} - x^2(\Psi)\right]^{1/2},\end{aligned} \tag{2}$$

where

$$I(\Psi) = \int_{-\infty}^{\infty}\Psi\Psi^*\mathrm{d}x \tag{3}$$

is proportional to the total intensity in the transversal plane and

$$x(\Psi) = \frac{1}{I(\Psi)}\int_{-\infty}^{\infty}\Psi\Psi^* x\mathrm{d}x \tag{4}$$

is the mean value of the transversal position of the beam. The factor 2 in Eq. (2) is introduced to obtain the Gaussian width ω when the equation is applied to a Gaussian beam. When $x(\Psi)$ is zero (not zero), we will say that the beam is on axis (off axis).

The divergence of a beam is the spread angle if the beam $\Psi(x)$ were permitted to evolve in free space up to the Fraunhofer region. It is related to the width of the Fourier transform of Ψ. Then if $\phi(\xi)$ denotes this Fourier transform, whose explicit expression is

$$\phi(\xi) = \int_{-\infty}^{\infty}\Psi(x)\exp(-i2\pi x\xi)\mathrm{d}x \tag{5}$$

where ξ is the transversal spatial frequency, we again define the beam divergence $\theta_0(\phi)$ by means of the MSD of $\phi\phi^*$:

$$\begin{aligned}\theta_0(\phi) &= 2\lambda\left\{\frac{\int_{-\infty}^{\infty}\phi\phi^*[\xi - \xi(\phi)]^2\mathrm{d}\xi}{I(\phi)}\right\}^{1/2} \\ &= 2\lambda\left[\frac{\int_{-\infty}^{\infty}\phi\phi^*\xi^2\mathrm{d}\xi}{I(\phi)} - \xi^2(\phi)\right]^{1/2},\end{aligned} \tag{6}$$

where $I(\phi)$ is defined as $I(\Psi)$ and

$$\xi(\phi) = \frac{1}{I(\phi)}\int_{-\infty}^{\infty}\phi\phi^*\xi\mathrm{d}\xi \tag{7}$$

is the mean value of the transversal spatial frequency. Parseval's theorem says that $I(\phi) = I(\Psi)$. The angle between the optical axis and the direction of the propagation of the beam is given by $\alpha = -\lambda\xi(\phi)$ (Ref. 14) within the paraxial approximation. Although the divergence is a far-field property, its value is implied in the field distribution at the transverse plane under consideration. This implication is the reason why we include the divergence, together with the width, as a property at this plane.

It is well known that the product of the width multiplied by the divergence cannot take arbitrary values.[15] The smallest permitted value for this product is λ/π. For Gaussian beams this limit is reached at the plane of smallest width ω_0 (the waist). Then, if we know the width of the waist, the divergence is given by $\theta_0 = \lambda/\pi\omega_0$. Thus divergence and width are dependent magnitudes for Gaussian beams. For any other non-Gaussian beam the value λ/π may not be reached along the entire evolution. In particular, at the transversal plane of smallest width $\omega_0(\Psi)$, the product $\omega_0(\Psi)\theta_0(\Psi)$ may be greater than λ/π, and the exact value for this product depends on the transversal intensity profile and wave front. This dependence means that we must consider width and divergence as two independent magnitudes for non-Gaussian beams. Therefore, the complex beam parameter for non-Gaussian beams will provide complete information if its definition takes into account both the divergence and the width. In fact, the imaginary part of the complex beam parameter for Gaussian beams, Eq. (1), can be understood as the quotient between the Gaussian divergence and the

Gaussian width if the waist were located at this plane ($\lambda/\pi\omega_1$ is not the divergence if ω_1 is not the waist width).

The next step is to define the curvature radius of a beam. Because its wave front is not generally spherical, we use the radius of the spherical wave front that best fits the actual one.

It is known that a quadratic phase

$$-\frac{k}{2R}(x - x_0)^2 + t, \tag{8}$$

with $k = 2\pi/\lambda$, represents a spherical wave front within the paraxial approximation. Its radius is R and the transversal position of its center is x_0. We must fit the phase of Ψ, $\arg(\Psi)$, to the phase of expression (8). Actually, we are not interested in the global phase t; therefore, we can differentiate expression (8) and $\arg(\Psi)$ with respect to x to obtain the linear fitting

$$[\arg(\Psi)]' \approx -\frac{k}{R}(x - x_0). \tag{9}$$

Now we apply the method of least squares. We are only interested in the wave-front curvature where the intensity distribution takes significant values, so the fitting has to be weighted with the intensity distribution. Thus we must find R and x_0 that minimize the expression

$$\int_{-\infty}^{\infty} \Psi\Psi^* \left\{[\arg(\Psi)]' + \frac{k}{R}(x - x_0)\right\}^2 \mathrm{d}x. \tag{10}$$

Differentiating with respect to R and x_0 and equating to zero, we obtain the following equations:

$$\frac{1}{2i}\int_{-\infty}^{\infty} (\Psi'\Psi^* - \Psi\Psi^{*\prime})(x - x_0)\mathrm{d}x + \frac{k}{R}\int_{-\infty}^{\infty} \Psi\Psi^*(x - x_0)^2\mathrm{d}x = 0, \tag{11}$$

$$\frac{1}{2i}\int_{-\infty}^{\infty} (\Psi'\Psi^* - \Psi\Psi^{*\prime})\mathrm{d}x + \frac{k}{R}\int_{-\infty}^{\infty} \Psi\Psi^*(x - x_0)\mathrm{d}x = 0, \tag{12}$$

where the following relations are used:

$$\Psi\Psi^*[\arg(\Psi)]' = \Psi\Psi^* \frac{\mathrm{d}}{\mathrm{d}x}\left[\tan^{-1}\frac{\mathrm{Im}(\Psi)}{\mathrm{Re}(\Psi)}\right] = \frac{1}{2i}(\Psi'\Psi^* - \Psi\Psi^{*\prime}). \tag{13}$$

Subtracting Eq. (12) multiplied by $[x(\Psi) - x_0]$ from Eq. (11), we remove x_0, and the value of the radius of the spherical wave front that best fits the actual wave front is obtained as

$$\frac{1}{R(\Psi)} = \frac{i\lambda}{\pi I(\Psi)\omega^2(\Psi)}\int_{-\infty}^{\infty} (\Psi'\Psi^* - \Psi\Psi^{*\prime}) \times [x - x(\Psi)]\mathrm{d}x. \tag{14}$$

The alternative expressions for the first moment of $\phi\phi^*$,

$$2\pi i\int_{-\infty}^{\infty} \phi\phi^*\xi\mathrm{d}\xi = \int_{-\infty}^{\infty} \Psi'\Psi^*\mathrm{d}x = -\int_{-\infty}^{\infty} \Psi\Psi^{*\prime}\mathrm{d}x, \tag{15}$$

allow us to rewrite Eq. (14) as

$$\frac{1}{R(\Psi)} = \frac{i\lambda}{\pi I(\Psi)\omega^2(\Psi)}\int_{-\infty}^{\infty} (\Psi'\Psi^* - \Psi\Psi^{*\prime})x\mathrm{d}x + \frac{4\lambda x(\Psi)\xi(\phi)}{\omega^2(\Psi)}. \tag{16}$$

Although the width is related with the mean values of the powers of x and the divergence with the mean values of the powers of ξ, we see from Eq. (14) or (16) that the expression for the radius involves the crossed products $x\xi$ (as in quantum mechanics, the differentiation of Ψ is equivalent to multiplying ϕ by ξ) and $x(\Psi)\xi(\phi)$.

Knowing the radius, we can obtain the transversal position of the center of the spherical wave front from Eqs. (12) and (15) as

$$x_0(\Psi) = x(\Psi) + \lambda\xi(\phi)R(\Psi) = x(\Psi) - \alpha R(\Psi). \tag{17}$$

Equation (17) means that the mean position of beam $x(\Psi)$ at the plane under study can be obtained from a ray coming from the center of the spherical wave front with slope α.

Formulas (2) for width, (6) for divergence, and (14) for radius are generalizations for non-Gaussian and nonspherical laser beams of the same magnitudes as for Gaussian beams. It is easy to prove that Eqs. (2), (6), and (14) give the usual Gaussian width, divergence, and radius of curvature when they are applied to a Gaussian beam. The generalized magnitudes are global properties of the beam. They do not exactly describe the shape of the beam, but they are mean magnitudes on the entire intensity profile and wave front. They are well defined when the mean values of $x^n\xi^m$, with $n + m \leq 2$, are finite.

Some examples may illustrate the variety of beam profiles for which the definitions given above apply. First we take the following beam with a finite lateral extent: $\Psi(x) = 1 - |x/b|$ for $|x| < b$, and $\Psi(x) = 0$ for $|x| \geq b$ (a triangular function). The width of this academic beam is $\sqrt{2/5}b$, i.e., the transversal distance at which the amplitude is 0.3675 times the amplitude on the axis (for Gaussian beams the amplitude decay at ω is 0.3679). The divergence is $\sqrt{3}\lambda/(\pi b)$, i.e., the point of 0.3247 decay of the central lobe in the

Fourier transform of Ψ, $b\,\mathrm{sinc}^2(b\xi)$. As Ψ is real its radius is infinite (the beam is plane). The product width times the divergence is $\sqrt{6/5}\lambda/\pi$, which is a little larger than λ/π. Now let us take a beam represented by a superposition of N HG modes:

$$\Psi(x) = \sum_{n=0}^{N-1} c_n \Psi_n(x; \omega), \tag{18}$$

with c_n a set of N complex numbers, and

$$\Psi_n(x; \omega) = \left(\frac{2}{\pi}\right)^{1/4} \frac{1}{(2^n n! \omega)^{1/2}} H_n\left(\frac{\sqrt{2}x}{\omega}\right) \exp\left(-\frac{x^2}{\omega^2}\right), \tag{19}$$

where only purely real HG modes are used for simplicity. Equation (18) can also represent the field at a plane inside the cavity, being the mode amplitudes c_n (possibly time dependent) given by the laser-cavity equations in simple cases. The Fourier transform of $\Psi(x)$, $\phi(\xi)$, is given by a similar superposition with coefficients $\tilde{c}_n = (-i)^n c_n$ and $\Psi_n(\xi; 1/\pi\omega)$ modes. A beam such as this usually has a few irregular ripples and always decays exponentially when $|x|$ increases. The same rule applies to its Fourier transform. Therefore, all the magnitudes defined in this section are well defined for this beam. Although $\omega(\Psi)$, $\theta_0(\phi)$, and $R(\Psi)$ can be determined directly from the profile and wave front of Ψ and from the profile of ϕ, it is interesting to express them in terms of the mode amplitudes c_n. Introducing $\Psi(x)$ given by Eq. (18) and $\phi(x)$ into Eqs. (2)–(7) and (14) and invoking the orthogonality, recurrence, and differential relations of the Ψ_n modes,[16] we find the mean position and slope as

$$x(\Psi) = \frac{\omega}{I(\Psi)} \mathrm{Re}\left[\sum_{n=0}^{N-1} c_n c_{n+1}^* \sqrt{n+1}\right], \tag{20}$$

$$\alpha = \frac{\lambda}{\pi\omega I(\phi)} \mathrm{Im}\left[\sum_{n=0}^{N-1} c_n c_{n+1}^* \sqrt{n+1}\right], \tag{21}$$

where

$$I(\Psi) = \sum_{n=0}^{N-1} |c_n|^2. \tag{22}$$

We find the width and the divergence as

$$\omega^2(\Psi) = \frac{\omega^2}{I(\Psi)}\left(\sum_{n=0}^{N-1} (2n+1)|c_n|^2 + 2\,\mathrm{Re}\left\{\sum_{n=0}^{N-1} [(n+1)(n+2)]^{1/2} c_n c_{n+2}^*\right\}\right) - 4x^2(\Psi), \tag{23}$$

$$\theta_0^2(\phi) = \frac{\lambda^2}{\pi^2\omega^2 I(\phi)}\left(\sum_{n=0}^{N-1} (2n+1)|c_n|^2 - 2\,\mathrm{Re}\left\{\sum_{n=0}^{N-1} [(n+1)(n+2)]^{1/2} c_n c_{n+2}^*\right\}\right) - 4\alpha^2, \tag{24}$$

and the radius as

$$\frac{1}{R(\Psi)} = \frac{\lambda}{\pi\omega^2(\Psi) I(\Psi)} \mathrm{Im}\left\{\sum_{n=0}^{N-1} [(n+1)(n+2)]^{1/2} \times (c_n c_{n+2}^* - c_{n+1} c_{n-1}^*)\right\} - \frac{4x(\Psi)\alpha}{\omega^2(\Psi)}. \tag{25}$$

In these expressions c_k are taken equal to zero if $k < 0$ or $k > N-1$. Equations (23) and (24) are a generalization of those in Ref. (9) for the width and divergence of only one HG mode. Among other things, these expressions say that the properties of the multimodal beam cannot be inferred in a simple way from the properties of the modes composing the beam. They depend strongly on how the modes are added up. For example, Eq. (25) shows how a superposition of plane HG modes can produce a beam with a net mean curvature; Eqs. (20) and (21) show how the off axis and the slope of a multimode beam are related to the presence of both even and odd transversal modes. As a particular case, let the c_n coefficients be uncorrelated random variables, i.e., $\Psi(x)$ is an incoherent mixture of HG modes. In this case the magnitudes of interest are the averages of $I(\Psi)$, $x(\Psi)$, $\xi(\phi)$, $\omega^2(\Psi)$, $\theta_0^2(\phi)$, and $R(\Psi)$ given by Eqs. (20)–(25). Assuming a uniform phase probability distribution for the c_n (caused, e.g., by Langevin noise), we see that the averages of any c_n and therefore of any crossed product $c_n c_k^*$, with $n \neq k$, are zero. The intensity pattern of this beam is the superposition of the intensity patterns of the HG modes weighted with $\langle |c_n|^2 \rangle$, where $\langle\ \rangle$ denotes ensemble average. From Eqs. (21) and (22) we see that the averaged mean transversal position and spatial frequency are zero. From Eq. (25) we see that the averaged radius is infinite, and from Eqs. (23) and (24) we see that the averaged width and divergence can be written as

$$\omega^2(\Psi) = \frac{\omega^2}{I(\Psi)} \sum_{n=0}^{N-1} (2n+1)\langle |c_n|^2 \rangle \equiv \omega^2 M, \tag{26}$$

$$\theta_0^2(\phi) = \frac{\lambda^2}{\pi^2\omega^2 I(\phi)} \sum_{n=0}^{N-1} (2n+1)\langle |c_n|^2 \rangle \equiv \frac{\lambda^2}{\pi^2\omega^2} M. \tag{27}$$

The product width times the divergence is then M times λ/π. This is a simple example of the so-called

M times diffraction-limited beams. For instance, when each c_n is a Gaussian random variable with variance σ and mean zero—the probability distribution is $P(c_n) = [1/(\pi\sigma^2)]\exp(-|c_n|^2/\sigma^2)$—it is found that $\langle |c_n|^2\rangle = \sigma^2$ and $M = N$, i.e., the beam is N times diffraction limited, where N is the number of modes.

These examples and the ones in Section 6 show how the magnitudes defined in this section permit us to express, in an analytical and useful way, properties of great interest, such as the width, divergence, or mean curvature of the wave front, for beams that do not have very much to do with the Gaussian beam. Now we will see how these magnitudes change when the beam is transformed by a real $ABCD$ optical system.

3. Transformation by a Real *ABCD* System

In a purely real $ABCD$ system, the beam is represented by $\Psi_1(x_1)$ at the input plane and by $\Psi_2(x_2)$ at the output plane (see Fig. 1). The generalized Huygens integral[17] for one transversal direction of an orthogonal system relates the output beam to the input one and the $ABCD$ elements

$$\Psi_2(x_2) = \sqrt{i/B\lambda}\int_{-\infty}^{\infty} \mathrm{d}x_1\Psi_1(x_1) \times \exp\left[-\frac{i\pi}{B\lambda}(Ax_1^2 - 2x_1x_2 + Dx_2^2)\right]. \quad (28)$$

An irrelevant phase factor depending on the length of the $ABCD$ system has been omitted. Because the elements of the $ABCD$ matrix are real numbers, the integrated intensity is invariant, $I(\Psi_1) = I(\Psi_2)$. Then, thanks to the Parseval's theorem, we can write without distinction $I(\Psi_1), I(\Psi_2), I(\phi_1)$, or $I(\phi_2)$.

As we may have expected, the mean values of the position, $x(\Psi)$, and the slope of the beam, $\alpha = -\lambda\xi(\phi)$, transform according to the geometrical optics rules when the beam passes through the $ABCD$ system:

$$\begin{bmatrix} x(\Psi_2) \\ -\lambda\xi(\phi_2)\end{bmatrix} = \begin{bmatrix} A & B \\ C & D\end{bmatrix}\begin{bmatrix} x(\Psi_1) \\ -\lambda\xi(\phi_1)\end{bmatrix}. \quad (29)$$

To see this transformation, we introduce Eq. (28) and its complex conjugate into the definition of the mean position, Eq. (4), for the output beam

$$x(\Psi_2) = \frac{1}{B\lambda I(\Psi_1)}\int_{-\infty}^{\infty}\int_{-\infty}^{\infty} \mathrm{d}x_1\mathrm{d}x_1'\Psi_1(x_1)\Psi_1^*(x_1') \times \exp\left[-\frac{i\pi}{B\lambda}A(x_1^2 - x_1'^2)\right] \times \int_{-\infty}^{\infty}\mathrm{d}x_2 x_2 \exp\left[\frac{2i\pi}{B\lambda}(x_1 - x_1')x_2\right]. \quad (30)$$

The integral in x_2 provides a first derivative of the Dirac δ function $\delta^{(1)}[(x_1 - x_1')/B\lambda]$. Then we can carry the integral in x_1 to obtain

$$x(\Psi_2) = \frac{A}{I(\Psi_1)}\int_{-\infty}^{\infty}\mathrm{d}x x\Psi_1(x)\Psi_1^*(x) - \frac{B\lambda}{I(\Psi_1)2\pi i}\int_{-\infty}^{\infty}\mathrm{d}x\Psi_1'(x)\Psi_1^*(x). \quad (31)$$

The first integral can be recognized as the input mean position, and the second is proportional to the input mean transversal spatial frequency [see Eq. (15)]. Then

$$x(\Psi_2) = Ax(\Psi_1) - B\lambda\xi(\phi_1) = Ax(\Psi_1) + B\alpha_1, \quad (32)$$

according to the geometrical transformation. The transformation of the mean transversal frequency is similar: We introduce the derivative of Eq. (28) with respect to x_2 and the complex conjugate of this equation into the alternative definition of the mean transversal spatial frequency given in Eq. (15). Then, following a similar method, we obtain

$$\alpha_2 = -\lambda\xi(\Psi_2) = Cx(\Psi_1) - D\lambda\xi(\phi_1) = Cx(\Psi_1) + D\alpha_1, \quad (33)$$

which completes the proof of Eq. (29).

For simplicity in the following calculations, we will assume that the beam is on axis and that its slope is zero at the input plane. This assumption means that $x(\Psi_1) = 0$ and $\xi(\phi_1) = 0$, and therefore, from Eq. (29), also $x(\Psi_2) = 0$ and $\xi(\phi_2) = 0$. It is not difficult to verify that all the results in this section remain valid in the general case of off-axis and tilted beams, $x(\Psi_1) \neq 0$ and $\xi(\phi_1) \neq 0$.

To find the width of the beam at the output plane, we introduce Eq. (28) and its complex conjugate into the definition of the width [Eq. (2) with $x(\Psi_2) = 0$] to obtain

$$\omega^2(\Psi_2) = \frac{4}{B\lambda I(\Psi_1)}\int_{-\infty}^{\infty}\int_{-\infty}^{\infty}\mathrm{d}x_1\mathrm{d}x_1'\Psi_1(x_1)\Psi_1^*(x_1') \times \exp\left[-\frac{i\pi}{B\lambda}A(x_1^2 - x_1'^2)\right] \times \int_{-\infty}^{\infty}\mathrm{d}x_2 x_2^2 \exp\left[\frac{2i\pi}{B\lambda}(x_1 - x_1')x_2\right]. \quad (34)$$

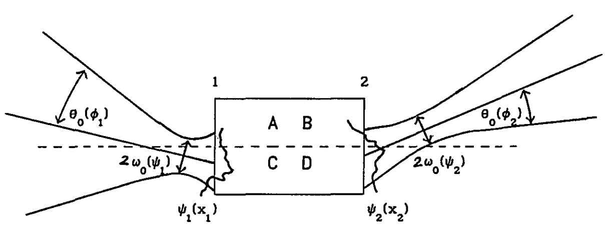

Fig. 1. Optical paraxial system illuminated by an arbitrary beam $\Psi_1(x_1)$. The $ABCD$ matrix elements are real, $\Psi_2(x_2)$ is the output beam, and $\theta_0(\phi_1)$, $\theta_0(\phi_2)$, $\omega_0(\Psi_1)$, and $\omega_0(\Psi_2)$ are the divergences and minimum widths of the input and output beams, respectively.

The integral in x_2 gives a second derivative of the Dirac δ, $\delta^{(2)}[(x_1 - x_1')/B\lambda]$. Then the integral in x_1 can be carried out:

$$\omega^2(\Psi_2) = \frac{4A^2}{I(\Psi_1)} \int_{-\infty}^{\infty} \mathrm{d}x x^2 \Psi_1(x)\Psi_1^*(x) - \frac{B^2\lambda^2}{I(\Psi_1)\pi^2} \times \int_{-\infty}^{\infty} \mathrm{d}x \Psi_1''(x)\Psi_1^*(x) + \frac{2i\lambda AB}{\pi I(\Psi_1)} \times \int_{-\infty}^{\infty} \mathrm{d}x[2\Psi_1^*(x)x\Psi_1'(x) + \Psi_1^*(x)\Psi_1(x)]. \tag{35}$$

The first integral in this expression gives the width of the input beam. The second one can be related to the input divergence by means of the first of the following identities,

$$-4\pi^2 \int_{-\infty}^{\infty} \phi^*\phi\xi^2 \mathrm{d}\xi = \int_{-\infty}^{\infty} \Psi^*\Psi'' \mathrm{d}x = \int_{-\infty}^{\infty} \Psi^{*\prime\prime}\Psi \mathrm{d}x = -\int_{-\infty}^{\infty} \Psi^{*\prime}\Psi' \mathrm{d}x, \tag{36}$$

and the third integral in Eq. (35) can be related to the input radius with the aid of

$$2\Psi_1^* x \Psi_1' + \Psi_1^*\Psi_1 = \Psi_1'\Psi_1^* x - \Psi_1\Psi_1^{*\prime} x + (\Psi_1\Psi_1^* x)'. \tag{37}$$

Then Eq. (35) becomes

$$\omega^2(\Psi_2) = A^2\omega^2(\Psi_1) + B^2\theta_0^2(\phi_1) + 2AB\frac{\omega^2(\Psi_1)}{R(\Psi_1)}, \tag{38}$$

and by adding and subtracting $B^2\omega^2(\Psi_1)/R(\Psi_1)$ we obtain

$$\omega(\Psi_2) = \omega(\Psi_1)\left\{\left[A + \frac{B}{R(\Psi)}\right]^2 + B^2\left[\frac{\theta_0^2(\phi_1)}{\omega^2(\Psi_1)} - \frac{1}{R^2(\Psi_1)}\right]\right\}^{1/2}, \tag{39}$$

which gives the width of the output beam when we know the width, divergence, and radius of the input one. This formula is similar to the one obtainable from the *ABCD* law for Gaussian beams. In fact, when Ψ_1 is Gaussian, $\omega(\Psi_1) = \omega_1$, $R(\Psi_1) = R_1$,

$$\theta_0(\phi_1) = \theta_0 = \frac{\lambda}{\pi\omega_0} = \frac{\omega_1}{R_1}\left[1 + \left(\frac{\lambda R_1}{\pi\omega_1^2}\right)^2\right]^{1/2}, \tag{40}$$

$$\left[\frac{\theta_0^2(\phi_1)}{\omega^2(\Psi_1)} - \frac{1}{R^2(\Psi_1)}\right]^{1/2} = \frac{\lambda}{\pi\omega_1^2}. \tag{41}$$

Therefore Eq. (39) reduces to the Gaussian width transformation.

In the case of free propagation ($A = D = 1$, $C = 0$, and $B = z$, with z being an axial coordinate), from Eq. (39) we find that the evolution of the width is hyperbolic as it is for Gaussian beams. The slope of the asymptotes is $\theta_0(\phi)$, as one may expect. Differentiating Eq. (39) with respect to z and equating to it zero, we find the position of the plane of the smallest width as

$$z_0(\Psi) = -\frac{\omega^2(\Psi_1)}{\theta_0^2(\phi_1)R(\Psi_1)}, \tag{42}$$

and this minimum width as

$$\omega_0^2(\Psi) = \omega^2(\Psi_1)\left[1 - \frac{\omega^2(\Psi_1)}{\theta_0^2(\phi_1)R^2(\Psi_1)}\right]. \tag{43}$$

The divergence of the beam at the output plane of an *ABCD* system, i.e., the far-field spread angle if the output beam is permitted to evolve up to the Fraunhofer region, can be obtained by making use of Eq. (36) to write the square of its definition [Eq. (6) with $\xi(\phi) = 0$] in terms of the first derivatives of Ψ_2 and Ψ_2^*:

$$\theta_0^2(\phi_2) = \frac{4\lambda^2}{I(\phi_2)} \int_{-\infty}^{\infty} \phi_2\phi_2^*\xi^2 \mathrm{d}\xi = \frac{\lambda^2}{\pi^2 I(\Psi_1)} \int_{-\infty}^{\infty} \Psi_2'(x_2)\Psi_2'^*(x_2)\mathrm{d}x_2. \tag{44}$$

Introducing into Eq. (44) the derivatives with respect to x_2 of Eq. (28) and its complex conjugate, we obtain

$$\theta_0^2(\phi_2) = \frac{4}{I(\Psi_1)} \frac{1}{B^3\lambda} \times \int_{-\infty}^{\infty}\int_{-\infty}^{\infty}\int_{-\infty}^{\infty} \mathrm{d}x_1\mathrm{d}x_1'\mathrm{d}x_2 \Psi_1(x_1)\Psi_1^*(x_1') \times (x_1x_1' - x_1x_2D - x_1'x_2D + Dx_2^2) \times \exp\left\{-\frac{i\pi}{B\lambda}[A(x_1^2 - x_1'^2) - 2(x_1 - x_1')x_2]\right\}. \tag{45}$$

After integrating in x_2, we can rewrite Eq. (45) as

$$\theta_0^2(\phi_2) = \frac{4}{I(\Psi_1)} \frac{1}{B^3\lambda} \int_{-\infty}^{\infty}\int_{-\infty}^{\infty} \mathrm{d}x_1\mathrm{d}x_1' \Psi_1(x_1)\Psi_1^*(x_1') \times \exp\left[-\frac{i\pi}{B\lambda}A(x_1^2 - x_1'^2)\right] \times \left[x_1x_1'\delta\left(\frac{x_1 - x_1'}{B\lambda}\right) - \frac{Dx_1}{2\pi i}\delta^{(1)}\left(\frac{x_1 - x_1'}{B\lambda}\right) - \frac{Dx_1'}{2\pi i}\delta^{(1)}\left(\frac{x_1 - x_1'}{B\lambda}\right) - \frac{D}{4\pi^2}\delta^{(2)}\left(\frac{x_1 - x_1'}{B\lambda}\right)\right]. \tag{46}$$

The integral with δ gives a term with the width of the input beam, and the integral with $\delta^{(2)}$ is similar to the one obtained in the width transformation. The integrals with $\delta^{(1)}$ are complexly conjugated. All of these properties permit us to write

$$\theta_0^2(\phi_2) = \frac{1}{B^2}\,\omega^2(\Psi_1) + \frac{D^2}{B^2}\,\omega^2(\Psi_2) - \frac{4}{I(\Psi_1)}\frac{1}{B^3\lambda}D \times \left\{\int_{-\infty}^{\infty}\int_{-\infty}^{\infty} \mathrm{d}x_1\mathrm{d}x_1{}'\Psi_1(x_1)\Psi_1{}^*(x_1{}') \times \exp\left[-\frac{i\pi}{B\lambda}A(x_1{}^2 - x_1{}'^2)\right] \times \frac{1}{2\pi i}\,\delta^{(1)}\left(\frac{x_1 - x_1{}'}{B\lambda}\right) + \mathrm{C.C.}\right\}, \tag{47}$$

where C.C. denotes the complex conjugate of the integral. Making the integral in x_1 or $x_1{}'$, we obtain

$$\theta_0^2(\phi_2) = \frac{1}{B^2}\,\omega^2(\Psi_1) + \frac{D^2}{B^2}\,\omega^2(\Psi_2) - \frac{2AD}{B^2}\,\omega^2(\Psi_1) - 2\,\frac{D}{B}\,\frac{\omega^2(\Psi_1)}{R(\Psi_1)}\cdot \tag{48}$$

By using Eq. (38) and taking into account that $AD - BC = 1$, we find that Eq. (48) becomes

$$\theta_0(\phi_2) = \omega(\Psi_1)\left\{\left[C + \frac{D}{R(\Psi_1)}\right]^2 + D^2\left[\frac{\theta_0^2(\phi_1)}{\omega^2(\Psi_1)} - \frac{1}{R^2(\Psi_1)}\right]\right\}^{1/2}, \tag{49}$$

which gives the output divergence (the far-field spread in the further free evolution of the output beam) as a function of the input beam parameters and the *ABCD* elements. Equations (39) and (49) look similar; they only differ in the elements of the *ABCD* matrix that they include (A, B or C, D), depending on the parameter that we are calculating. For the free evolution along z, we can see from Eq. (49) that the divergence is invariant because the Fourier transform ϕ is only shifted in a phase factor along the free evolution.

Following the same method, we can derive the expression for the radius transformation from Eqs. (14) [with $x(\Psi) = 0$] and Eq. (28) [here it is useful to note that $\Psi'\Psi^* - \Psi\Psi^{*\prime} = 2i\,\mathrm{Im}(\Psi'\Psi^*)$]:

$$\frac{1}{R(\Psi_2)} = \frac{\omega^2(\Psi_1)}{\omega^2(\Psi_2)}\left\{\left[A + \frac{B}{R(\Psi_1)}\right]\left[C + \frac{D}{R(\Psi_1)}\right] + BD\left[\frac{\theta_0^2(\phi_1)}{\omega^2(\Psi_1)} - \frac{1}{R^2(\Psi_1)}\right]\right\}, \tag{50}$$

which gives the mean curvature radius of the wave front. In the case of free propagation, one finds $R(\Psi_2)$ equal to infinity and the beam is almost plane when the plane of minimum width is the output plane. Formula (50) also reduces to the usual formula for Gaussian beams, deducible from the real part of the *ABCD* law, when it is applied to a Gaussian beam.

From the transformation of the mean values $x(\Psi)$ and $\xi(\phi)$ found in Eq. (29) and from the general definitions of the width, divergence, and radius found in Eqs. (2), (6), and (16), it is easy to prove that the three transformation formulas, Eqs. (39), (49), and (50), are also valid when $x(\Psi_1) \neq 0$ and $\xi(\phi_1) \neq 0$. This validity means that in the paraxial approximation the behavior of the width, divergence, and radius through *ABCD* systems is independent of the transversal position and slope of the beam with respect to the optical axis.

Take the case of an almost plane beam [$R(\Psi_1) = \infty$] focused by a lens of focal length f. The transformation formulas let us obtain the characteristics of the beam just behind the lens as $\omega^2(\Psi_2) = \omega^2(\Psi_1)$, $R(\Psi_2) = -f$, and $\theta_0^2(\phi_2) = \theta_0^2(\phi_1) + \omega^2(\Psi_1)/f^2$. Substituting these values into Eq. (42), we obtain the axial point behind the lens with the smallest MSD and with the most plane wave front, $z_0(\Psi)$. It is convenient to express it as

$$\frac{z_0(\Psi) - f}{f} = -\frac{1}{1 + [\omega(\Psi_1)/\theta_0(\phi_1)f]^2}, \tag{51}$$

which is a generalization of the focal shift formula for Gaussian beams. From Eq. (43) we can see that the absolute value of Eq. (51) provides the quotient between the smallest and the input widths, $\omega_0^2(\Psi)/\omega^2(\Psi_1)$.

Let us again consider a general beam Ψ, including off-axis and tilted beams. Now we are interested in the meaning of the expression

$$\left[\frac{\theta_0^2(\phi)}{\omega^2(\Psi)} - \frac{1}{R^2(\Psi)}\right]^{1/2}, \tag{52}$$

which appears in the three transformation formulas, Eqs. (39), (49), and (50). For Gaussian beams Eq. (52) should give [see Eq. (41)] the divergence θ_0 divided by the width ω_1 if the waist width were ω_1. If one collimates the beam at this plane, e.g., with a lens, the waist width should be ω_1 and expression (52) should be the quotient of the divergence and the waist width. This interpretation remains valid for non-Gaussian laser beams. Let us consider the beam

$$\Psi_p = \Psi\exp\left[i\,\frac{k}{2R(\Psi)}\,x^2\right]. \tag{53}$$

This beam can be obtained by passing Ψ through a converging thin lens of focal length $f = R(\Psi)$. We can determine the characteristics of Ψ_p by means of the transformation formulas for this lens. The mean position and the width remain unchanged. The radius of Ψ_p is infinite, i.e., its average wave front is plane where the intensity is significant because one has collimated the beam by means of the phase factor of Eq. (53) (see Fig. 2). The slope of the beam is also

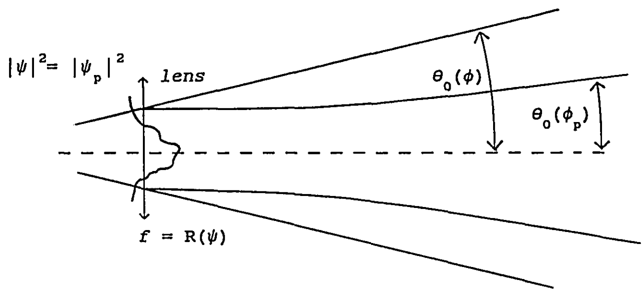

Fig. 2. Divergence $\theta_0(\phi)$ of the beam $\Psi(x)$ and divergence $\theta_0(\Psi_p)$ of the collimated beam $\Psi p(x)$. An on-axis and nontilted beam is depicted for clarity.

changed, $\alpha_p = \alpha - x(\Psi)/R(\Psi)$, and finally the divergence of Ψ_p is given by

$$\theta_0(\phi_p) = \left[\theta_0{}^2(\phi) - \frac{\omega^2(\Psi)}{R^2(\Psi)}\right]^{1/2}. \tag{54}$$

Expression (52) then gives the divergence divided by the width of the collimated beam.

We already have seen a conserved quantity in the propagation of a light beam: The integrated intensity $I(\Psi)$ does not change if the elements of the matrix $ABCD$ are real. Another invariant is the product of $\theta_0(\phi_p)$ times the width $\omega(\Psi)$. By combining transformation formulas (39), (49), and (50) and after some calculation, we obtain the following relation:

$$\omega(\Psi_1)\left[\theta_0{}^2(\phi_1) - \frac{\omega^2(\Psi_1)}{R^2(\Psi_1)}\right]^{1/2} = \omega(\Psi_2)\left[\theta_0{}^2(\phi_2) - \frac{\omega^2(\Psi_2)}{R^2(\Psi_2)}\right]^{1/2}. \tag{55}$$

This product can be calculated at the input plane, at the output plane, or at any plane after the $ABCD$ system because the free evolution also preserves this quantity. If we do this at the real or virtual planes of minimum width of the input and output beams [$R(\Psi_1) = R(\Psi_2) = \infty$], Eq. (55) means that the product of the smallest width times the divergence is invariant. As we have seen in Section 2, the conserved quantity is λ/π for Gaussian beams. For other beams it is greater than λ/π but remains unchanged after arbitrary $ABCD$ transformations for a given laser beam.

The knowledge of the value of the invariant product of Eq. (55) for a given laser beam is useful. A simple method for measuring this invariant is as follows. First, collimate the beam at an arbitrary plane, which is easy experimentally; second, measure the width and the divergence of the collimated beam; third, multiply them. Once the invariant product is known, it permits us to obtain the curvature radius $R(\Psi)$ at a given plane of interest only by measuring the divergence and the width at this plane and by using Eq. (55).

Now we will use this conserved product and the transformation formulas to deduce the $ABCD$ law for non-Gaussian beams.

4. Complex Beam Parameter and *ABCD* Law for Non-Gaussian Beams

Let us define the following complex magnitude:

$$\frac{1}{q(\Psi)} = \frac{1}{R(\Psi)} - i\left[\frac{\theta_0{}^2(\phi)}{\omega^2(\Psi)} - \frac{1}{R^2(\Psi)}\right]^{1/2} = \frac{1}{R(\Psi)} - i\,\frac{\theta_0(\phi_p)}{\omega(\Psi)}. \tag{56}$$

Its real part is the curvature radius and its imaginary part is the divergence divided by the width of the collimated beam. From the first equality in Eq. (56), one may think that the imaginary part of $1/q(\Psi)$ depends on the radius and therefore on the wave front. However, the second equality means that it only depends on the collimated beam. When the fitting between the spherical and the real wave fronts is fine, one may expect the divergences of Ψ_p (plane in average) and $|\Psi| = \sqrt{\Psi\Psi^*}$ (exactly plane) to be equal. In this case, the imaginary part of $1/q(\Psi)$ can be computed by means of the square root of the intensity profile and its Fourier transform.

Let us write

$$\frac{C + D/q(\Psi_1)}{A + B/q(\Psi_1)}, \tag{57}$$

where $q(\Psi_1)$ is the magnitude defined in Eq. (56) for the beam $\Psi_1(x_1)$ inciding on an $ABCD$ system. Multiplying and dividing by the complex conjugate of the denominator, we find the real part of expression (57) as the inverse of the output radius, $1/R(\Psi_2)$, and the imaginary part as the divergence divided by the width of the output collimated beam, $-\theta_0(\phi_{p2})/\omega(\Psi_2)$. Then expression (57) is equal to $1/q(\Psi_2)$. Taking its inverse and multiplying and dividing by $q(\Psi_1)$, we see that $q(\Psi)$ changes according to the $ABCD$ law:

$$q(\Psi_2) = \frac{Aq(\Psi_1) + B}{Cq(\Psi_1) + D}. \tag{58}$$

Therefore we will name $q(\Psi)$ as the complex beam parameter of the beam. Equation (58) is the $ABCD$ law for any (orthogonal) laser beam, provided that the magnitudes defined in Section 2 are well defined.

From the $ABCD$ law and the conservation law [Eq. (55)] one can again deduce the width, divergence, and radius transformations. Note that by using only the $ABCD$ law, which provides only two equations from their real and imaginary parts, it is not possible to deduce the transformation formulas. The conservation law is the third condition necessary to solve this system: Let $K(\Psi_1)$ be the invariant product for the input beam. The conservation law establishes that $K(\Psi_1) = K(\Psi_2)$ [see Eq. (55)]. Equating the real parts of the two members of the generalized *ABCD* law, we obtain $R(\Psi_2)$ as Eq. (50). The imaginary part provides $K(\Psi_2)/\omega^2(\Psi_2)$, which is equal to $K(\Psi_1)/\omega^2(\Psi_2)$. Then a value of $\omega(\Psi_2)$ like the one in Eq. (39) is obtained. Finally, a value of $\theta_0(\phi_2)$ like that of Eq. (49) can be obtained from the conservation law $K(\Psi_1) = K(\Psi_2)$.

5. Cylindrical Symmetric Beams

This section and Appendix A are brief repetitions of Sections 2 and 3 for cylindrical symmetric beams passing through cylindrical symmetric *ABCD* systems. All the results, including the conservation law, Eq. (55), and the extended *ABCD* law, Eq. (58), remain valid in this case.

For cylindrical symmetric beams it is useful to write all the magnitudes in polar coordinates (r, θ). The integrated intensity in the transversal plane is

$$I(\Psi) = \int_0^{2\pi} \mathrm{d}\theta \int_0^{\infty} \Psi(r)\Psi^*(r) r \mathrm{d}r = 2\pi \int_0^{\infty} \Psi(r)\Psi^*(r) r \mathrm{d}r. \tag{59}$$

The width of the beam is twice the two-dimensional MSD in any direction,[18]

$$\omega(\Psi) = 2\left[\frac{1}{I(\Psi)}\int_0^{2\pi} \cos^2\theta \mathrm{d}\theta \int_0^{\infty} \Psi(r)\Psi^*(r) r^3 \mathrm{d}r\right]^{1/2} = 2\left[\frac{\pi}{I(\Psi)}\int_0^{\infty} \Psi(r)\Psi^*(r) r^3 \mathrm{d}r\right]^{1/2}, \tag{60}$$

and the radius of curvature is the value of R that minimizes the expression

$$\int_0^{2\pi}\int_0^{\infty}\left\{[\arg\Psi(r)]' + \frac{k}{R}r\right\}^2 r\mathrm{d}r\mathrm{d}\theta, \tag{61}$$

where the prime denotes differentiation with respect to r. Differentiating with respect to R, one finds

$$\frac{1}{R(\Psi)} = \frac{i\lambda}{I(\Psi)\omega^2(\Psi)}\int_0^{\infty} (\Psi'\Psi^* - \Psi\Psi^{*\prime}) r^2 \mathrm{d}r, \tag{62}$$

which is the average radius of curvature of the wave front along any transversal direction. The divergence is defined by the two-dimensional MSD along any direction of the spatial frequency plane,

$$\theta_0(\phi) = 2\lambda\left[\frac{\pi}{I(\phi)}\int_0^{\infty} \phi(\rho)\,\phi^*(\rho)\rho^3 \mathrm{d}\rho\right]^{1/2}, \tag{63}$$

where ρ is the radial polar coordinate in the spatial frequency plane.

Now the *ABCD* matrix represents a paraxial optical system with cylindrical symmetry. In such a case the amplitude distribution at the output plane is given by the generalized Huygens integral for cylindrical symmetric systems,[3] which is essentially a zero-order Hankel transformation of the input beam

$$\Psi_2(r_2) = i\frac{2\pi}{\lambda B}\int_0^{\infty} \Psi_1(r_1)\exp\left[-\frac{i\pi}{\lambda B}(Ar_1^2 + Dr_2^2)\right] \times r_1 J_0\left(\frac{2\pi r_1 r_2}{\lambda B}\right)\mathrm{d}r_1, \tag{64}$$

where J_0 is the Bessel function of the first kind and zero order.

The procedure for obtaining the width, divergence, and radius at the output plane as a function of the input ones is similar to the orthogonal case, and the details are given in Appendix A. It is seen from this appendix that the three transformation formulas are identical to the orthogonal case, and therefore the conservation and the *ABCD* law remain valid for cylindrical symmetric beams.

6. Examples

A. Super-Gaussian Beams

To illustrate the cylindrical symmetric case and the formalism in general, we consider the family of functions $\Psi_s(r) = \exp(-r^s/\omega^s)$, where s is a real number larger than or equal to 2. These functions represent the beam profile of some lasers for fusion experiments (e.g., with $s = 5$).[5] To interpret the values of the width, divergence, and radius of these beams, we first need to take a look at Ψ_s and its Fourier transform ϕ_s. For $s = 2$ the beam is Gaussian. When s increases Ψ_s becomes more and more squared, and in the limit Ψ_∞ is the circular hard aperture of radius ω. The far-field patterns $\phi_s\phi_s^*$ have a big central maximum with small sidelobes surrounding them for all s. The central maximum stretches with s, but only a little. The limit is the central maximum of the Airy pattern corresponding with the circular aperture of radius ω. The fractional power in the central maximum decreases with s (until 0.838), and therefore the fractional power in the sidelobes increases with s (until 0.162). However, the values of the intensity distributions in the sidelobes are always very small in comparison with the peak intensities (lower than 0.0175 for all s). Some of the intensity distributions, $\Psi_s\Psi_s^*$ and $\phi_s\phi_s^*$, can be seen in Figs. 3(a) and (b).

These beams, usually high-power beams, accumulate a self-induced wave-front distortion by passing through the laser medium. This effect is the so-called whole-beam self-focusing effect. Under certain conditions[7] this aberration is proportional to the intensity profile,

$$\Psi_s^{(a)}(r) = \Psi_s(r)\exp(-ikL|\Psi_s(r)|^2), \tag{65}$$

where L (always greater than zero) is the magnitude

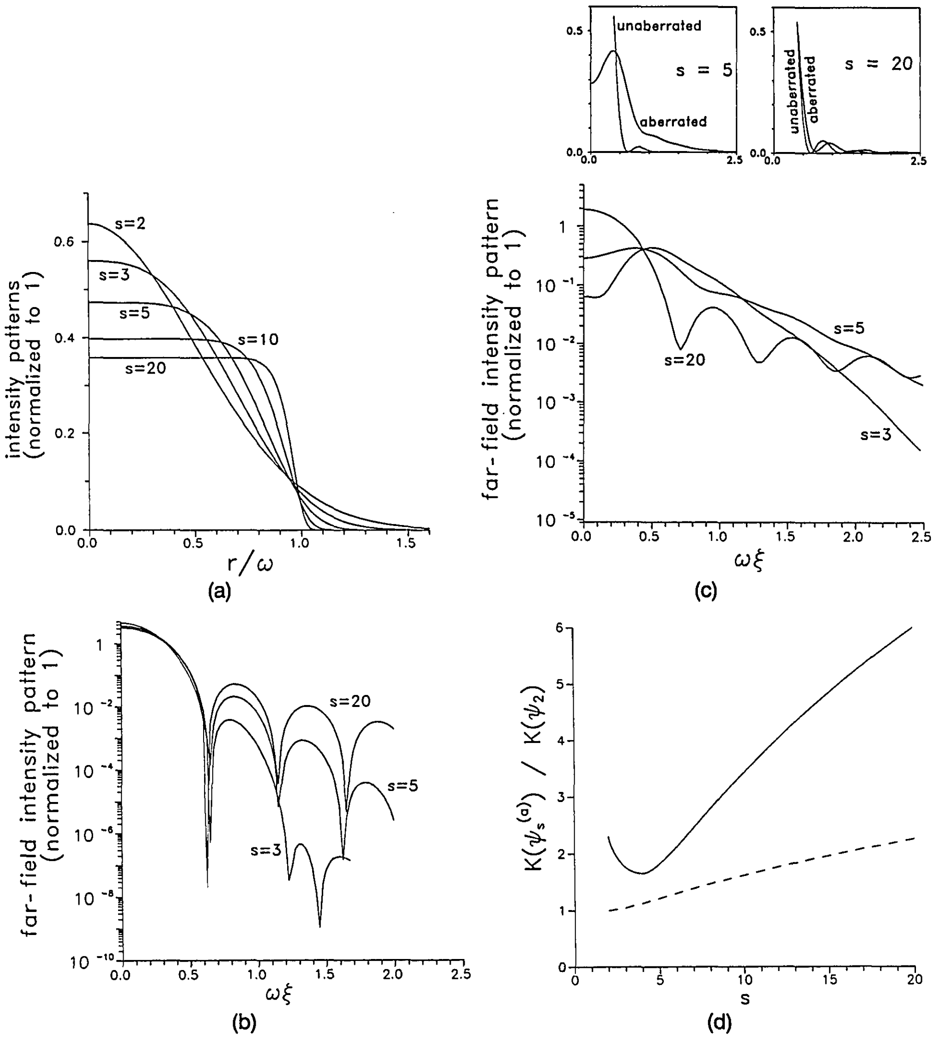

Fig. 3. (a) Intensity profiles of some Ψ_s and $\Psi_s^{(a)}$. (b) Some far-field intensity patterns of the unaberrated beams ϕ_s and (c) of the aberrated beams $\phi_s^{(a)}$. These patterns are shown in logarithmic scale for best viewing of the sidelobes. On the top of (c) the comparison between aberrated and unaberrated far-field patterns is shown in lineal scale. (d) Conserved products for the Ψ_s beams (dashed curve) and for the $\Psi_s^{(a)}$ beams (solid curve) as a function of s. The magnitude of the aberration is $L = 0.75\lambda$.

of the phase distortion. Although the intensity profiles of both the aberrated and unaberrated beams are identical for all s, their far-field patterns are different enough for small and moderate values of s (e.g., $s < 20$). In contrast, the phase aberration of Eq. (65) becomes a constant phase kL as $|\Psi_s(r)|^2$ tends to the circular hard aperture, i.e., the aberration tends to disappear for large s and the Fourier transforms $\phi_s^{(a)}$ tend to ϕ_s. Figure 3(c) shows some far-field intensity distributions for the aberrated case, $\phi_s^{(a)}\phi_s^{(a)*}$. The top of this figure shows how the aberration fairly modifies the far-field pattern for low s and how the effect of the aberration is much weaker for $s = 20$.

The parameters of these beams can be calculated with an appropriate table of integrals.[19] The widths of both Ψ_s and $\Psi_s^{(a)}$ are given by

$$\omega^2(\Psi_s) = \frac{2^{2/s}}{\sqrt{\pi}}\,\Gamma\left(\frac{2}{s} + \frac{1}{2}\right)\omega^2, \tag{66}$$

where Γ is the Euler gamma function; the divergences are given by

$$\theta_0^2(\phi_s) = \frac{s^2 2^{2/s}}{8\Gamma(2/s)}\frac{\lambda^2}{\pi^2\omega^2},$$

$$\theta_0^2(\phi_s^{(a)}) = \theta_0^2(\phi_s)\left[1 + \left(\frac{2kL}{3}\right)^2\right], \tag{67}$$

and the radii are given by

$$\frac{1}{R(\Psi_s)} = 0, \qquad \frac{1}{R(\Psi_s^{(a)})} = \frac{-2\sqrt{\pi}}{2^{4/s}\Gamma[(2/s) + (1/2)]\omega^2}L. \tag{68}$$

Then the conserved products $K(\Psi) = \omega(\Psi)[\theta_0^2(\phi) - \omega^2(\Psi)/R^2(\Psi)]^{1/2}$ are

$$K^2(\Psi_s) = \frac{\lambda^2}{\pi^2}\frac{s^2}{4}\frac{\Gamma(4/s)}{\Gamma^2(2/s)}, \tag{69}$$

$$K^2(\Psi_s^{(a)}) = K^2(\Psi_s)\left\{1 + \left(\frac{2kL}{3}\right)^2\left[1 - \left(\frac{3}{2^{2/s}s}\right)^2\frac{\Gamma^2(2/s)}{\Gamma(4/s)}\right]\right\}. \tag{70}$$

The values of $\omega(\Psi)$ are slightly lower than ω for $s > 2$ because of the faster decay of these functions when r increases. The divergences of the unaberrated beams are always greater than the Gaussian divergence and they increase as $\sqrt{s}$ for large s. This growth is first due to the small enlargement of the central maximum of ϕ_s and second to the growth of the sidelobes with s. The only effect of the aberration on the divergence is to multiply it by a constant factor greater than one, which can be written as $1 + (2kL/3)^2$. The wave front of the unaberrated beam is plane because Ψ_s is real. The aberration, besides increasing the divergence, is taken into account like a mean curvature of the wave front that is proportional to the magnitude of the aberration [Eq. (68)]. Then the transformation formula of the width for the free evolution shows that the aberrated beams will reach an axial point of minimum width given by Eq. (43), explaining the self-focusing of these beams.

Equations (69) and (70) may be understood as a measure of the removal of these beams from the Gaussian beam optimum behavior. We see that $K(\Psi_s)$ is greater than λ/π for $s > 2$; as the divergence, it grows as $\sqrt{s}$. The conserved products $K[\Psi_s^{(a)}]$ for the aberrated beams with $L = 0.75\ \lambda$ as a function of s can be seen in Fig. 3(d). This figure can explain the use of the profiles represented by Ψ_s, with s larger than 2, in the presence of this type of aberration. Two factors are at work for the value of $K[\Psi_s^{(a)}]$. The first is the loss of quality caused by the increase of the energy in the sidelobes; the second is the loss of quality caused by the aberration. The first factor becomes important for large s, and the second for low s. For $s \simeq 4$ (when $L = 0.75\ \lambda$) $K[\Psi_s^{(a)}]$ reaches a minimum value, which must be understood as a commitment between these two opposite factors.

B. Truncated Gaussian Beam

The last example is the free evolution of a truncated Gaussian beam. We have said before that the MSD of the Fourier transform of these types of beams is not well defined. This would mean that the *ABCD* law and the conservation laws derived in this paper would no longer apply in a strict sense. However, let us fix the scope of these laws from a more realistic point of view. First we have to establish the physical meaning of the concepts of convergence and divergence when they are applied to magnitudes involving integration over the whole plane, such as the width, divergence, and radius.

Physically speaking, only the integrals over a finite area are measurable. Then the convergence of the width, divergence, and radius means that the value of the corresponding integrals over the whole plane can be approximated with arbitrarily adjustable accuracy by means of the measured, or numerically calculated, integrals over a finite area. Obviously the precision increases as the integration area contains more and more of the beam intensity. Therefore, we can conclude that the *ABCD* law and the conservation law are exact laws to transform the theoretical magnitudes, $\omega(\Psi)$, $\theta_0(\phi)$, and $R(\Psi)$, which are defined by means of an infinite area of integration; furthermore, their results are arbitrarily close to the exact ones when these laws are applied to the transformation of the previous magnitudes measured or evaluated over a finite integration area.

The divergence of $\omega(\Psi)$, $\theta_0(\phi)$, or $R(\Psi)$ means that the value of any one of these magnitudes is arbitrary and unbounded, depending on the size of the integration domain. This undetermination disappears if we specify a criterion to define the integration domain. In spite of this, we cannot state any generalized conclusion about the validity of the transformation laws when they deal with these magnitudes defined over a finite area. Nevertheless, we can expect a certain degree of approximation to the *ABCD* law and the conservation law when the integration areas contain most of the energy of the beam.

A weakly truncated[9] cylindrical Gaussian beam has been studied as an example in which one of the magnitudes, the divergence, diverges. For a weakly truncated beam the power loss in the truncation is small, but the diffraction effects are still significant (see Ref. 9). In particular, the near-field patterns are different enough from the Gaussian beam, showing significant Fresnel ripples. To simplify the calculation and the physical situation of the problem, we assume that the beam has its waist on the aperture plane. Actually we have chosen an input Gaussian width of $\omega_0 = 1$ mm, truncated by an aperture whose radius is $a = \sqrt{2}$ mm, and with a wavelength of $\lambda = 0.6328 \times 10^{-3}$ mm. The Fresnel integral has been used for evaluating the free evolution behind the aperture plane. This exact calculation allows us to obtain the values of the width of the beam, $\omega(\Psi)$, and the radius of curvature of the wave front, $R(\Psi)$, at several planes. In contrast, the divergence $\theta_0(\phi)$ has been evaluated at the spatial frequency plane. To obtain these previous magnitudes, we have carried out the integration over a circular integration area containing a known encircled energy in the spatial frequency plane by using the exact amplitude distribution. The amount of encircled energy has been used like a constant parameter to determine the integration limits on the planes behind the aperture, where we have calculated the width and the radius of curvature following a conservative criterion.

The adequate values for the encircled energy must be greater than 99.3% for this particular beam. This value determines an integration domain containing only the central maximum of the Fourier transform.

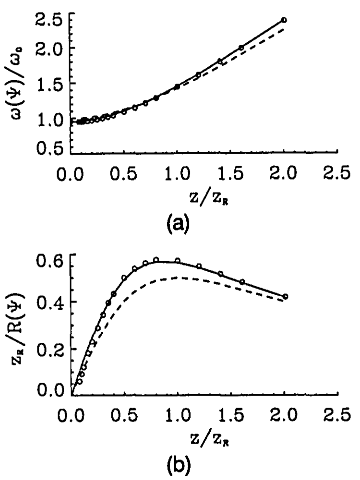

Fig. 4. Evolution of the (a) width and (b) radius of curvature of the diffracted Gaussian beam: ω_0 is the width of the input Gaussian beam and z_R is its Rayleigh range. The open circles are numerical data, based on the Fresnel integral, with a 99.4% criterion; the solid curve is the *ABCD* law prediction; the dashed curve is the evolution of the nondiffracted Gaussian beam.

A lower value would partially exclude the outer region of the central maximum and would not provide a correct evaluation of the divergence. In contrast, values greater than 99.3% can be chosen if we include some of the rings of the Fourier transform in the integration area. For instance, if we take into account both the central maximum and the first ring to evaluate the divergence, then 99.4% of the total energy will be encircled.

Figure 4(a) shows the evolution of the width of the diffracted beam. The open circles represent the numerical data obtained by means of the Fresnel integral when the calculation uses the 99.4% criterion. The solid curve shows the behavior predicted by the *ABCD* law:

$$\omega^2(\Psi) = \omega^2(\Psi_0)\left[1 + z^2 \frac{\theta_0{}^2(\phi_0)}{\omega^2(\Psi_0)}\right], \qquad (71)$$

where z is the axial coordinate and $\omega(\Psi_0)$ and $\theta_0(\phi_0)$ are the width and divergence of the truncated Gaussian beam computed with the 99.4% criterion just behind the aperture plane ($z = 0$). The maximum relative error between the *ABCD* law prediction and the numerical data is lower than 1% in the region between $N = 9$ and $N = 0.3$, where $N = a^2/z\lambda$ is the Fresnel number. Besides, we have found that the maximum error follows an inverse relation with respect to the fractional power within the integration domain (1.2% error for the 99.3% criterion and 0.7% for the 99.6% criterion).

Figure 4(b) shows the evolution of the averaged radius of curvature of the diffracted beam. Here again the open circles are the numerical data for the 99.4% criterion and the solid curve is the *ABCD* law evolution,

$$R(\Psi) = z\left[1 + \frac{\omega^2(\Psi_0)}{z^2\theta_0{}^2(\phi_0)}\right]. \qquad (72)$$

A measure of the validity of this formula can be represented by the phase difference between the spherical wave fronts of radius $R(\Psi)$ when the radius is obtained from Eq. (72) or from the numerical data. The maximum error always occurs at the edge of the integration domain $r_{\max}$ (i.e., the maximum error is given by $|\tfrac{1}{2}kr_{\max}{}^2[1/R(\Psi) - 1/R_N(\Psi)]|$, where $R_N(\Psi)$ are the numerical data). After evaluating this error at several positions along the z axis, we found that it lies between 0.003π and 0.03π rad. In addition, this error is similar for several similar criteria. This fact has to be interpreted as an actual growth of the accuracy as the fractional power increases, i.e., the error remains constant regardless of the growth of $r_{\max}$ with the fractional power. The difference between both of the spherical wave fronts at the edge of the integration domain is approximately constant although this domain stretches, i.e., $R(\Psi)$ approaches $R_N(\Psi)$ as the fractional power increases.

We also have calculated the value of the product $K^2(\Psi) = \{\theta_0{}^2(\phi) - [\omega^2(\Psi)/R^2(\Psi)]\}\omega^2(\Psi)$, which remains almost constant in the free propagation after the aperture. The actual value for this example is $K(\Psi) = (1.027 \pm 0.007)(\lambda/\pi)$ when the 99.4% criterion is chosen. The maximum relative variation, $\Delta K(\Psi)/\overline{K(\Psi)}$ (where the overbar denotes the mean value along the propagation axis), remains lower than 2, 1.5, and 1% for the 99.3, 99.4, and 99.6% criteria, respectively, again showing an increase of the accuracy with the fractional power. At the same time the magnitudes involved in the definition of K show big changes in wide ranges ($\Delta R(\Psi)/\overline{R(\Psi)} \approx 400\%$ and $\Delta\omega(\Psi)/\overline{\omega(\Psi)} \approx 100\%$).

The detailed study of this example shows how the *ABCD* law and the conservation law still represent, with a high degree of accuracy, the transformation of the width, divergence, and radius of curvature, at least for the free propagation of a weakly truncated Gaussian beam. The procedure explained in this section is necessary for truncated beams and in general when the width, divergence, or radius diverge. It can also be applied when the three magnitudes converge if we modify the integration region by removing the areas without physical interest as widespread energy. In this case we will lose accuracy in the transformation laws but we will improve the characterization of the beam.

7. Conclusions

We have studied the propagation of non-Gaussian and nonspherical light beams through paraxial optical systems. We have investigated the whole behavior of the beam without considering the exact intensity profile and wave front. To do this we needed to define the width, divergence, and radius of curvature for non-Gaussian and nonspherical beams. The complex beam parameter for this type of beams has been defined by involving the three previous magnitudes. The formulas of transformation of the width, divergence, and radius of curvature show that they represent the immediate generalizations of the same magnitudes for Gaussian beams.

We have used the generalized Huygens integral to prove that the new complex beam parameter changes according to the *ABCD* law when an orthogonal or cylindrical symmetric beam is transformed by a real *ABCD* system. The *ABCD* law is also valid for off-axis and tilted beams. We have found that the product of the minimum width, $\omega_0(\Psi)$, times the divergence at the same plane, $\theta_0(\phi)$, is conserved by any *ABCD* transformation. To evaluate the conserved product at any plane along the propagation of the beam, we find that it is necessary to collimate the beam, measure its width and divergence, and finally multiply them. This invariant product allows us to classify the light beams according to its value. In particular, beams with $\omega_0(\Psi)\theta_0(\phi) = \lambda/\pi$ (minimal beams) are Gaussian beams or beams whose global behavior is reducible to the Gaussian case. Beams with $\omega_0(\Psi)\theta_0(\phi) > \lambda/\pi$ (nonminimal) are essentially different from Gaussian beams, and it is not possible to find a Gaussian beam that evolves, with regard to its width, divergence, and radius, as a nonminimal beam.

We have applied the results to some typical laser beams. From the *ABCD* law and the conservation law it is possible to deduce algebraic and useful fomulas that yield an adequate description of the laser-beam properties of interest. By using an example we have seen how the method presented in this paper can be applied to truncated beams.

Finally, the further developments, consequences, and particular cases of the usual *ABCD* law (paraxial resonator theory, circle diagrams, optical systems design, Gaussian beams in lenslike media, misaligned systems, etc.) can be reinterpreted for non-Gaussian beams by using the extended *ABCD* law and the complex beam parameter defined here.

Appendix A

Here we deduce the formulas of transformation of the width, divergence, and radius when a cylindrical symmetric beam incides on a cylindrical symmetric *ABCD* system.

We can obtain the width at the output plane of the system as a function of the input parameters by substituting Eq. (64) and its conjugate into Eq. (60):

$$\begin{aligned}\omega^2(\Psi_2) = {}& \frac{8\pi^2}{\lambda^2 B^2 I(\Psi_1)} \int_0^\infty\int_0^\infty \mathrm{d}r_1 \mathrm{d}r_1' r_1 r_1' \Psi_1(r_1)\Psi_1^*(r_1') \\ & \times \exp\left[-\frac{i\pi}{\lambda B} A(r_1^2 - r_1'^2)\right] \\ & \times 2\pi \int_0^\infty r_2^2 J_0\left(\frac{2\pi r_1 r_2}{\lambda B}\right) J_0\left(\frac{2\pi r_1' r_2}{\lambda B}\right) r_2 \mathrm{d}r_2. \end{aligned} \tag{A1}$$

The integral in r_2 can be identified[8] with the zero-order Hankel transform of $r_2^2 J_0(2\pi r_1 r_2/\lambda B)$ that gives two terms with the first and second derivative of the δ function:

$$\begin{aligned}\omega^2(\Psi_2) = {}& \frac{-1}{\pi\lambda^2 B^2 I(\Psi_1)} \int_0^\infty\int_0^\infty \mathrm{d}r_1 \mathrm{d}r_1' r_1 r_1' \Psi_1(r_1)\Psi_1^*(r_1') \\ & \times \exp\left[-\frac{i\pi}{\lambda B} A(r_1^2 - r_1'^2)\right] \\ & \times \frac{\lambda B}{r_1}\left[\delta^{(2)}\left(\frac{r_1' - r_1}{\lambda B}\right) + \frac{\lambda B}{r_1'}\delta^{(1)}\left(\frac{r_1' - r_1}{\lambda B}\right)\right]. \end{aligned} \tag{A2}$$

The δ functions allow us to carry out the integral in r_1' to yield

$$\begin{aligned}\omega^2(\Psi_2) = {}& \frac{1}{\pi I(\Psi_1)}\Bigg\{-\lambda^2 B^2 \int_0^\infty \Psi_1(r)\Psi_1^{*\prime}(r)\mathrm{d}r \\ & - \lambda^2 B^2 \int_0^\infty \Psi_1(r)\Psi_1^{*\prime\prime}(r) r\mathrm{d}r \\ & - 4\pi i\lambda AB \int_0^\infty [\Psi_1(r)\Psi_1^{*\prime}(r) r + \Psi_1(r)\Psi_1^*(r)] \\ & + 4\pi^2 A^2 \int_0^\infty \Psi_1(r)\Psi_1^*(r) r^3 \mathrm{d}r\Bigg\}. \end{aligned} \tag{A3}$$

The identity

$$(r^2\Psi\Psi^*)' = 2r\Psi\Psi^* + r^2\Psi'\Psi^* + r^2\Psi\Psi^{*\prime} \tag{A4}$$

allows us to identify the radius in the third integral of Eq. (A3). The first two integrals in Eq. (A3) are related to the divergence of the input beam by means of the identity

$$-4\pi^2 \int_0^\infty \phi\phi^*\rho^3 \mathrm{d}\rho = \int_0^\infty \Psi\Psi^{*\prime}\mathrm{d}r + \int_0^\infty \Psi\Psi^{*\prime\prime} r\mathrm{d}r, \tag{A5}$$

and the last integral in Eq. (A3) gives the width of the input beam. One then finds the formula for the width transformation, Eq. (39), given in Section 3. Because the width for cylindrical symmetric beams is also the width in the x direction, the meaning of Eq. (39) for orthogonal astigmatic and for cylindrical beams is the same.

The radius of the output beam can be obtained by differentiating Eq. (64) with respect to r_2 to obtain

$$\begin{aligned}\Psi_2'(r_2) = {}& \frac{4\pi^2}{\lambda^2 B^2} \int_0^\infty \Psi_1(r_1) r_1 \left[r_2 D J_0\left(\frac{2\pi r_1 r_2}{\lambda B}\right)\right. \\ & \left. - i r_1 J_1\left(\frac{2\pi r_1 r_2}{\lambda B}\right)\right] \exp\left[-\frac{i\pi}{\lambda B}(A r_1^2 + D r_2^2)\right] \mathrm{d}r_1. \end{aligned} \tag{A6}$$

With this derivative and the complex conjugate of

Eq. (64), we can write

$$\int_0^\infty \Psi_2'(r_2)\Psi_2^*(r_2)r_2^2 \mathrm{d}r_2 = -\frac{8\pi^3 i}{\lambda^3 B^3}\int_0^\infty\int_0^\infty \mathrm{d}r_1\mathrm{d}r_1' r_1 r_1'$$
$$\times \Psi_1(r_1)\Psi_1^*(r_1')\exp\left[-\frac{i\pi}{\lambda B}A(r_1^2 - r_1'^2)\right]$$
$$\times \int_0^\infty \mathrm{d}r_2 r_2^2 \left[D r_2 J_0\left(\frac{2\pi r_1 r_2}{\lambda B}\right)J_0\left(\frac{2\pi r_1' r_2}{\lambda B}\right)\right.$$
$$\left. - i r_1 J_1\left(\frac{2\pi r_1 r_2}{\lambda B}\right)J_0\left(\frac{2\pi r_1' r_2}{\lambda B}\right)\right]. \tag{A7}$$

The integral with the first term in the square bracket is similar to that in Eq. (A1), providing a term with the output width. The integral in r_2 with the second term in the square bracket gives[18]

$$2\pi \int_0^\infty \mathrm{d}r_2 r_2^2 J_1\left(\frac{2\pi r_1 r_2}{\lambda B}\right)J_0\left(\frac{2\pi r_1' r_2}{\lambda B}\right)$$
$$= \frac{r_1}{4\pi^2 \lambda B}\left[\delta^{(1)}\left(\frac{r_1' - r_1}{\lambda B}\right) + \frac{\lambda B}{r_1'}\delta\left(\frac{r_1' - r_1}{\lambda B}\right)\right]. \tag{A8}$$

Then the integral in r_1' in Eq. (A7) can be carried out to obtain

$$\int_0^\infty \Psi_2'(r_2)\Psi_2^*(r_2)r_2^2 \mathrm{d}r_2 = -i\frac{D}{2\lambda B}I(\Psi_1)\omega^2(\Psi_2)$$
$$+ \int_0^\infty \mathrm{d}r r^2 \Psi_1(r)\Psi_1^{*\prime}(r)$$
$$+ \frac{2\pi i A}{\lambda B}\int_0^\infty \mathrm{d}r r^3 \Psi_1(r)\Psi_1^*(r). \tag{A9}$$

Introducing this equation and its complex conjugate into the definition of the radius, Eq. (62), we find

$$\frac{1}{R(\Psi_2)} = \frac{D}{B} - \frac{\omega^2(\Psi_1)}{\omega^2(\Psi_2)R(\Psi_1)} - \frac{A}{B}\frac{\omega^2(\Psi_1)}{\omega^2(\Psi_2)}. \tag{A10}$$

Factoring $\omega^2(\Psi_1)/\omega^2(\Psi_2)$, using Eq. (38) for $\omega(\Psi_2)$, adding and subtracting $DB\omega^2(\Psi_1)/R^2(\Psi_1)\omega^2(\Psi_2)$, and taking into account that $AD - BC = 1$, we obtain Eq. (50). By the same method it is easy to prove that the divergence of the output beam is given by Eq. (49).

The three transformation formulas are identical for orthogonal and radial symmetric beams. Therefore the conservation and the *ABCD* laws remain valid in the last case.

M. A. Porras acknowledges the suppport of the Ministerio de Educacion y Ciencia of Spain. He is also most grateful to the other authors for their support. J. Alda's stay at the Center for Research in Electro-Optics and Lasers was supported by a grant from the center and by the Programa de Perfeccionamiento y Movilidad del Personal Investigador, BE90-140, Dirección General de Investigación Científica y Tecnológica.

Note added in proof: A similar *ABCD* law that applies to orthogonal, on-axis, and untilted beams was also derived by P. A. Bélanger [Opt. Lett. **16,** 196–198 (1991)].

References and Notes

1. H. Kogelnik, "Imaging of optical mode-resonators with internal lenses," Bell Syst. Tech. J. **44,** 455–494 (1965).
2. H. Kogelnik and T. Li, "Laser beams and resonators," Proc. IEEE **54,** 1312–1329 (1966).
3. J. P. Taché, "Derivation of the *ABCD* law for Laguerre–Gaussian beams," Appl. Opt. **26,** 2698–2700 (1987).
4. S. G. Roper, "Beam divergence of a highly multimode CO_2 laser," J. Phys. E **11,** 1102–1103 (1978).
5. J. T. Hunt, P. A. Renard, and W. W. Simmons, "Improved performance of fusion lasers using the imaging properties of multiple spatial filters," Appl. Opt. **16,** 779–782 (1977).
6. C. B. Hogge, R. R. Butts, and M. Burlakoff, "Characteristics of phase-aberrated nondiffraction-limited laser beams," Appl. Opt. **13,** 1065–1070 (1974).
7. J. T. Hunt, P. A. Renard, and R. G. Nelson, "Focusing properties of an aberrated laser beam," Appl. Opt. **15,** 1458–1464 (1976).
8. J. P. Campbell and L. G. DeShazer, "Near fields of truncated-Gaussian apertures," J. Opt. Soc. Am. **59,** 1427–1429 (1969).
9. P. Belland and J. P. Crenn, "Changes in the characteristics of a Gaussian beam weakly diffracted by a circular aperture," Appl. Opt. **21,** 522–527 (1982).
10. W. H. Carter, "Spot size and divergence for Hermite–Gaussian beams of any order," Appl. Opt. **19,** 1027 (1980).
11. R. L. Phillips and L. C. Andrews, "Spot size and divergence for Laguerre Gaussian beams of any order," Appl. Opt. **22,** 643–644 (1983).
12. F. Gori, M. Santarsiero, and A. Sona, "The change of the width for a partially coherent beam on paraxial propagation," Opt. Commun. **82,** 197–203 (1991).
13. J. Alda, S. Wang, and E. Bernabeu, "Analytical expression for the complex radius of curvature tensor Q for generalized Gaussian beams," Opt. Commun. **80,** 350–352 (1991).
14. The most usual definition of the Fourier transform is with the minus in the exponential (see Ref. 18 below). In addition, in paraxial wave optics the most usual definition of the plane wave traveling toward positive x is with the minus in the exponential (see Ref. 17 below). The consequence of these choices is the minus in this expression.
15. P. A. Bélanger and P. Mathieu, "On an extremum property of Gaussian beams and Gaussian pulses," Opt. Commun. **67,** 396–398 (1988).
16. A. E. Siegman and E. A. Sziklas, "Mode calculations in unstable resonators with flowing saturable gain. 1: Hermite–Gaussian expansion," Appl. Opt. **13,** 2775–2791 (1974).
17. A. E. Siegman, *Lasers,* (Oxford U. Press, Mill Valley, Calif., 1986), pp. 777–782.
18. J. D. Gaskill, *Linear Systems, Fourier Transforms and Optics* (Wiley, New York, 1978), pp. 323–330.
19. S. M. Selby, ed., *Standard Mathematical Tables* (CRC, Boca Raton, Fla., 1972), p. 449.